North-Central Pacific Tropical Cyclones: Impacts of El Niño–Southern Oscillation and the Madden–Julian Oscillation

PHILIP J. KLOTZBACH

Department of Atmospheric Science, Colorado State University, Fort Collins, Colorado

ERIC S. BLAKE

National Hurricane Center, National Oceanic and Atmospheric Administration, Miami, Florida

(Manuscript received 17 November 2012, in final form 14 March 2013)

ABSTRACT

Both El Niño–Southern Oscillation (ENSO) and the Madden–Julian oscillation (MJO) have been documented in previous research to impact tropical cyclone (TC) activity around the globe. This study examines the relationship of each mode individually along with a combined index on tropical cyclone activity in the north-central Pacific. Approximately twice as many tropical cyclones form in the north-central Pacific in El Niño years compared with La Niña years. These differences are attributed to a variety of factors, including warmer sea surface temperatures, lower sea level pressures, increased midlevel moisture, and anomalous midlevel ascent in El Niño years. When the convectively enhanced phase of the MJO is located over the eastern and central tropical Pacific, the north-central Pacific tends to have more tropical cyclone activity, likely because of reduced vertical wind shear, lower sea level pressures, and increased vertical motion. The convectively enhanced phase of the MJO is also responsible for most of the TCs that undergo rapid intensification in the north-central Pacific. A combined MJO–ENSO index that is primarily associated with anomalous rising motion over the tropical eastern Pacific has an even stronger relationship with north-central Pacific TCs, as well as rapid intensification, than either individually.

1. Introduction

El Niño–Southern Oscillation (ENSO) is a coupled mode of oceanic and atmospheric variability that has been shown to alter the global climate (Rasmussen and Carpenter 1982). El Niño events are associated with warmer-than-normal sea surface temperatures (SSTs) in the eastern and central equatorial Pacific. Along with these SST anomalies are fluctuations in the strength and location of the Walker circulation (Wang 2005), which impact broad-scale areas of ascent–descent as well as upper- and lower-level winds. These fluctuations have been shown to alter tropical cyclone (TC) frequency around the globe (e.g., Camargo et al. 2007). In the tropical eastern North Pacific basin, Gray and Sheaffer (1991) showed that major hurricane activity was increased in El Niño years, with reduced TC activity in La Niña years. Collins (2010) has shown, when splitting the eastern North Pacific basin at 116°W, that El Niño significantly increases TC activity in the western part of the basin but has little impact on the eastern part of the basin. Chu (2004) has documented an increase in TC activity in the north-central Pacific in El Niño years.

The Madden–Julian oscillation (MJO; Madden and Julian 1972) is a large-scale mode of tropical variability that propagates around the globe on an approximately 30–60-day time scale. As it moves, the MJO alters magnitudes of vertical motion, vertical wind shear, midlevel moisture, and sea level pressure (SLP) fields, among others. These alterations have been implicated as to why TCs tend to cluster in time around the globe, as observed by Gray (1979) and more recently by Camargo et al. (2009). The relationship between the MJO and eastern Pacific TCs was discussed by Maloney and Hartmann (2000), Aiyyer and Molinari (2008), and Barrett and Leslie (2009). Maloney and Hartmann (2000) documented that when low-level westerly wind anomalies associated with the MJO were present in the eastern Pacific, TC activity was enhanced. Aiyyer and Molinari (2008) noted

Corresponding author address: Philip J. Klotzbach, Department of Atmospheric Science, Colorado State University, Fort Collins, CO 80523.
E-mail: philk@atmos.colostate.edu

DOI: 10.1175/JCLI-D-12-00809.1

FIG. 1. TC statistics for the central North Pacific basin by year from 1974 to 2010. (top) Named storms (NS; pink bar), hurricanes (H; blue bar), and major hurricanes (MH; green bar). Mean (median) values of these parameters from 1974 to 2010 are 2.8 (2.0) NS, 1.2 (1.0) H, and 0.5 (0.0) MH, respectively. (middle) Named storm days (NSD; pink bar), hurricane days (HD; blue bar), and major hurricane days (MHD; green bar). Mean (median) values of these parameters from 1974–2010 are 10.7 (8.0) NSD, 4.0 (2.8) HD, and 1.1 (0.0) MHD, respectively. (bottom) Accumulated cyclone energy ($10^4\,kt^{-2}$; where $1\,kt = 0.51\,m\,s^{-1}$). Mean (median) value of this parameter for 1974–2010 is 17.8 (13.2).

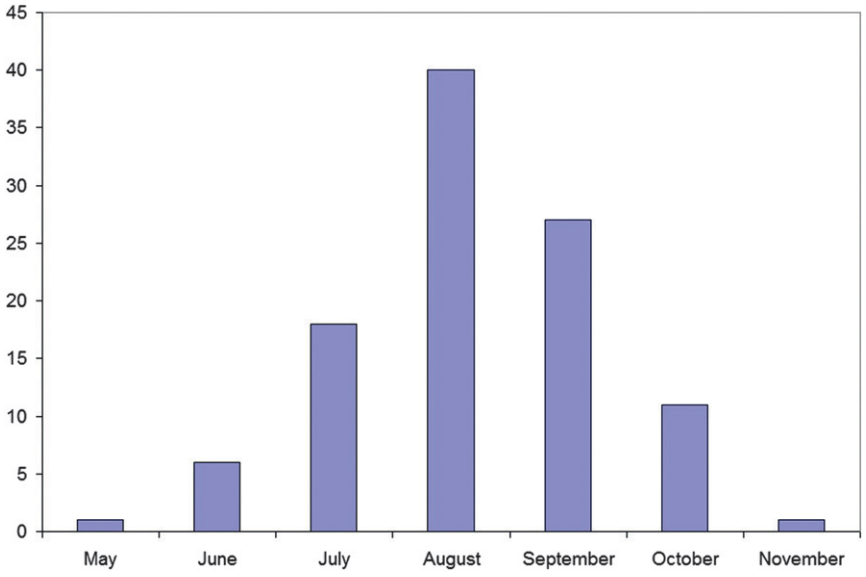

FIG. 2. Named storm formations per month during the north-central Pacific hurricane season for 1974–2010.

significant enhancement of eastern Pacific TCs followed by enhancement of Gulf of Mexico TCs during an enhanced MJO event from late August through mid-September 1998. Barrett and Leslie (2009) focused on upper-level anomalies as measured by 200-mb velocity potential and documented an increase in eastern and north-central Pacific TCs when negative 200-mb velocity potential anomalies were centered near 120°W (indicative of anomalous upper-level divergence).

Given these relationships, it is hypothesized that a combined MJO–ENSO index could have a significant relationship with TCs in the north-central Pacific (defined in this paper as from 120°W to 180° and north of the equator). Klotzbach (2012) showed that when a combined MJO–ENSO index developed by Wheeler and Hendon (2004) favored anomalous ascent over the Indian Ocean, it was associated with very active periods for Atlantic basin TC formation as well as increasing the likelihood for rapid intensification (RI). When the anomalous ascent occurred over the western tropical Pacific, both the formation likelihood and the RI frequency of Atlantic TCs decreased significantly.

This paper examines the relationship between ENSO and the MJO with north-central Pacific TCs, first individually and then using a combined index. Section 2 discusses the data utilized in this manuscript, while section 3 examines the climatology of TCs forming in the north-central Pacific. Section 4 describes how ENSO modulates TC activity in the north-central Pacific, while section 5 documents how the MJO modulates TC activity in the north-central Pacific. Section 6 examines how a combined MJO–ENSO index impacts TC activity in the north-central Pacific. Section 7 summarizes the manuscript and provides some ideas for future work.

2. Data

As in Klotzbach (2012), the Multivariate ENSO Index (MEI) was utilized to classify ENSO events (Wolter and Timlin 1998). This index uses six atmospheric–oceanic

TABLE 1. Classification of years by ENSO phase based upon the June–October-averaged MEI index. Average MEI values are provided in parentheses. The 10 years with the highest (lowest) MEI values since 1974 were classified as El Niño (La Niña) years; all other years were classified as neutral.

El Niño	Neutral	La Niña
1977 (+0.84)	1976 (+0.81)	1974 (−0.76)
1982 (+1.82)	1979 (+0.60)	1975 (−1.78)
1986 (+0.84)	1980 (+0.40)	1988 (−1.38)
1987 (+1.81)	1981 (+0.04)	1989 (−0.39)
1991 (+0.94)	1983 (+0.81)	1996 (−0.38)
1993 (+1.03)	1984 (−0.10)	1998 (−0.43)
1994 (+0.96)	1985 (−0.31)	1999 (−0.83)
1997 (+2.77)	1990 (+0.20)	2007 (−0.78)
2002 (+0.81)	1992 (+0.67)	2008 (−0.44)
2009 (+0.91)	1995 (−0.25)	2010 (−1.76)
	2000 (−0.25)	
	2001 (+0.04)	
	2003 (+0.31)	
	2004 (+0.52)	
	2005 (+0.22)	
	2006 (+0.76)	

TABLE 2. June–October average values of SST (°C), SLP (mb), 200-mb zonal wind U ($m\,s^{-1}$), 850-mb U ($m\,s^{-1}$), 200–850-mb U (zonal shear; $m\,s^{-1}$), 700-mb relative humidity (RH; %), 500-mb omega ($mb\,day^{-1}$), and OLR ($W\,m^{-2}$) averaged across the main development region (MDR). Differences between El Niño and La Niña that are statistically significant at the 5% level are highlighted in boldface type.

	SST	SLP	200-mb U	850-mb U	200–850-mb U	700-mb RH	500-mb omega	OLR
El Niño	27.6	1012.0	2.6	−5.1	7.7	44.1	−10.1	248.4
Neutral	27.3	1012.5	2.9	−5.2	8.1	41.2	−6.4	252.5
La Niña	27.0	1013.0	2.7	−5.3	8.0	40.1	−0.7	257.0
El Niño–La Niña	**0.6**	**−1.0**	−0.1	0.2	−0.3	**4.0**	**9.4**	**−8.6**

factors (sea level pressure, zonal and meridional components of the surface wind, SST, surface air temperature, and total cloud fraction) to classify ENSO events and generally is considered to be a more comprehensive metric of ENSO events than simply using an SST index such as Niño-3.4. Since we are primarily interested in the atmospheric response to an ENSO event as opposed to simply the ENSO-associated SST anomaly, we find the MEI more useful index for our analysis. The MEI index uses a bimonthly average; for this analysis, the bimonthly averages of June–July, July–August, August–September, and September–October are averaged together to classify ENSO events.

The daily phase of the MJO was determined using the technique outlined in Wheeler and Hendon (2004, hereafter WH) and available online (http://cawcr.gov.au/staff/mwheeler/maproom/RMM/RMM1RMM2.74toRealtime.txt). They utilized a multivariate EOF analysis to isolate the signal of the MJO by analyzing upper- and lower-level zonal winds along with outgoing longwave radiation (OLR). The two principal component (PC) time series that make up the WH MJO index are referred to as Real-Time Multivariate MJO series 1 and 2 (RMM1 and RMM2). Their index is constructed by first removing the 120-day mean along with interannual variability associated with large-scale phenomena such as ENSO. This index is available from 1974 to the present, with data missing for most of 1978 due to issues with observations of OLR.

TABLE 3. Average number per year of NS, NSD, H, HD, MH, MHD, and ACE observed for each phase of ENSO. The El Niño–La Niña ratio is also provided. Ratio differences that are statistically significant at the 5% level are highlighted in boldface type, while ratio differences that are statistically significant at the 10% level are highlighted in italics.

	NS	NSD	H	HD	MH	MHD	ACE
El Niño	4.3	16.5	2.0	5.6	0.8	1.8	27.9
Neutral	2.3	8.4	0.9	3.2	0.4	0.8	13.7
La Niña	1.9	7.2	0.9	2.9	0.3	0.6	11.8
El Niño/La Niña ratio	**2.5**	*2.6*	*2.6*	*2.2*	2.5	2.7	*2.6*

An additional index is available from WH that is similar but includes the 120-day mean and interannual variability associated with ENSO. This index is available online (http://cawcr.gov.au/staff/mwheeler/maproom/RMM/createdPCs.TotAnom.74toRealtime.txt) and is referred to as the WH-Combined index for the remainder of this manuscript. This index is useful for including the impacts of ENSO on large-scale vertical motion patterns. For both the original MJO index and the WH-Combined index, only days when the respective index is greater than or equal to one $[(RMM1^2 + RMM2^2)^{0.5} \geq 1]$ are considered. The MJO index is greater than one for approximately 60% of all days during June–October. For the remaining 40% of days, the MJO may not be a significant contributing factor to intraseasonal TC variability. Alternatively, the RMM signal may be getting interfered with by other modes of equatorial wave variability, such as Kelvin waves or equatorial Rossby waves. For example, a strong equatorial Kelvin wave may be projecting on the 850-mb zonal wind component in the Indian Ocean, while the 200-mb zonal wind component associated with the MJO is located over the western Pacific.

Large-scale field calculations were made based on the National Centers for Environmental Prediction (NCEP)–National Center for Atmospheric Research (NCAR) Reanalysis (Kistler et al. 2001) except for OLR. OLR was calculated from the National Oceanic and Atmospheric Administration (NOAA) Interpolated OLR dataset (Liebmann and Smith 1996).

In this paper, the north-central Pacific was defined to be north of the equator and to extend from 180° to 120°W, instead of to 140°W as defined by the World Meteorological Organization. As noted in the introduction, Collins

TABLE 4. Percentage of TCs forming in the north-central Pacific achieving at least one 24-h period of RI of 25+, 30+, 35+, and 40+ kt, respectively, given various phases of ENSO.

	RI (25+ kt)	RI (30+ kt)	RI (35+ kt)	RI (40+ kt)
El Niño	38	38	27	18
Neutral	39	22	17	6
La Niña	44	39	22	17

TABLE 5. TC activity generated by storms forming in each phase of the MJO. All values are normalized by the number of days that the MJO spends in a particular phase for June–October 1974–2010 and are multiplied by 100. Differences that are statistically significant at the 10% and 5% level using a two-tailed Student's *t* test between phases 7 and 8 and phases 4 and 5 are highlighted in the ratio row in italics and boldface, respectively.

Phase	NS	NSD	H	HD	MH	MHD	ACE
1	1.6	7.6	0.9	3.0	0.3	0.8	12.5
2	0.8	4.1	0.8	2.6	0.4	0.6	9.2
3	1.7	8.1	1.4	3.2	0.0	0.0	10.6
4	1.2	3.2	0.3	0.4	0.0	0.0	2.8
5	1.5	4.1	0.2	1.2	0.2	0.5	6.2
6	2.4	7.3	0.2	0.7	0.2	0.1	7.1
7	3.0	12.6	1.5	5.9	1.1	3.2	32.2
8	2.9	12.6	1.9	6.0	0.6	0.7	20.7
Average	1.9	7.5	0.9	2.9	0.4	0.7	12.7
Phases 7 and 8	2.9	12.6	1.7	6.0	0.9	1.9	26.0
Phases 4 and 5	1.4	3.8	0.2	0.9	0.1	0.3	4.9
Phases 7 and 8/phases 4 and 5 ratio	*2.1*	**3.3**	**7.5**	**6.6**	*7.5*	6.6	**5.3**

(2010) demonstrated a significant difference in TC frequency during ENSO events by utilizing 116°W as a boundary in the eastern North Pacific, and the breakdown used here is close to her longitudinal breakdown. In addition, there is a large increase in sample size that occurs by including 20 additional degrees of longitude. Only 30 TCs of tropical storm strength or greater occurred during 1974–2010 west of 140°W, while 104 TCs occurred during 1974–2010 west of 120°W. For the remainder of this manuscript, we define TC to be for tropical cyclones that have at least a maximum sustained wind of 34 kt. The year 1974 was used as the starting year because of MJO index availability beginning that year.

North-central Pacific TC statistics were computed from the Atlantic basin hurricane database (HURDAT; Davis et al. 1984). HURDAT provides 6-hourly information on storm location and intensity. All TCs that are first classified as a named storm (greater than or equal to 34-kt maximum 1-min sustained wind) in the eastern North Pacific basin west of 120°W are considered to be north-central Pacific storms. TC statistics are then tabulated until the storm dissipates or crosses the International Date Line. Statistics for RI are calculated only for TCs that had a wind speed at or above 34 kt at the start of the RI period; that is, systems that underwent a 24-h RI period with initial strength as a tropical depression were excluded. This methodology helps to prevent issues with tropical depression classifications. RI is calculated over a 24-h period, with thresholds for RI of 25, 30, 35, and 40+ knots examined in this manuscript.

To test statistical significance of the results found in this manuscript, a two-tailed Student's *t* test is utilized. The Student's *t* test is robust when the distribution is approximately normal; however, there can be problems

TABLE 6. June–October anomalous values calculated over the north-central Pacific MDR for SST (°C), SLP (mb), 200-mb U ($m\,s^{-1}$), 850-mb U ($m\,s^{-1}$), 200–850-mb U ($m\,s^{-1}$), 700-mb RH (%), 500-mb omega ($mb\,day^{-1}$), and OLR ($W\,m^{-2}$) across the north-central Pacific MDR. Differences between MJO phases 7 and 8 and phases 4 and 5 that are statistically significant at the 5% level are highlighted in boldface type in the difference row.

MJO phase	SST	SLP	200-mb U	850-mb U	200–850-mb U	700-mb RH	500-mb omega	OLR
1	−0.01	0.19	−2.98	1.42	−4.40	−1.91	4.28	6.11
2	−0.05	0.20	−1.74	0.59	−2.33	−2.11	3.71	5.59
3	−0.04	0.06	0.77	−0.65	1.42	−2.04	2.66	5.62
4	0.00	−0.17	3.15	−1.34	4.48	−1.20	−1.20	0.29
5	0.05	−0.28	2.47	−1.52	3.99	1.00	−5.52	−6.67
6	0.00	−0.11	1.70	−0.78	2.48	1.75	−4.45	−7.61
7	0.04	−0.04	−0.63	0.53	−1.17	5.08	0.09	−5.62
8	0.02	0.13	−2.07	1.81	−3.88	1.44	0.39	1.55
Phases 7 and 8	0.03	0.04	−1.35	1.17	−2.53	3.26	0.24	−2.04
Phases 4 and 5	0.02	−0.23	2.81	−1.43	4.24	−0.10	−3.36	−3.19
Phases 7 and 8 − phases 4 and 5	0.01	0.27	**−4.16**	**2.60**	**−6.76**	**3.36**	3.60	1.15

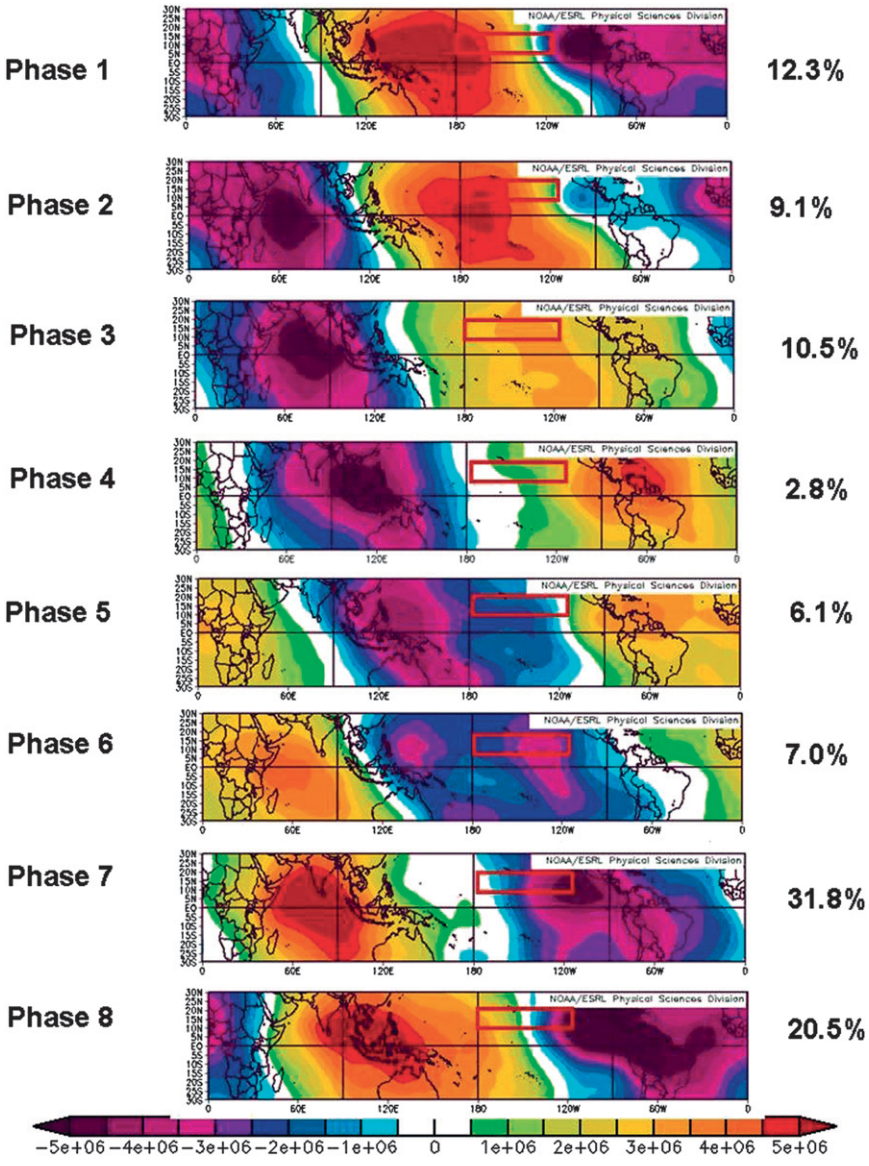

FIG. 3. Velocity potential anomalies ($m^2 s^{-1}$) at the 0.21 sigma level for all days for June–October when the MJO was greater than one for (from top to bottom) each phase of the MJO. Numbers on the rhs represent the percentage of normalized ACE generated by TCs forming in each phase of the MJO. The red box represents the north-central Pacific MDR (8°–18°N, 180°–120°W).

when the data are skewed. Because of this, a one-sided Wilcoxon–Mann–Whitney (WMW) nonparametric test in the direction indicated by the Student's *t* test is also conducted. Significance of results is shown utilizing the *t* test, and significance using the one-sided WMW test is mentioned in the text. Each individual year is counted as one degree of freedom, while a conservative estimate of 50 degrees of freedom is counted for the MJO. The MJO occurs approximately every 40–60 days, and 35 years are being examined in this manuscript.

3. North-central Pacific TC climatology

Figure 1 displays various TC statistics in the north-central Pacific over the period from 1974 to 2010. All TC statistics except for accumulated cyclone energy (ACE) are defined as in Klotzbach and Gray (2003), with ACE as defined in Bell et al. (2000). In the north-central Pacific, over the period 1974–2010, approximately 43% of TCs that developed became hurricanes at some point during their lifetime. This number is slightly less than for

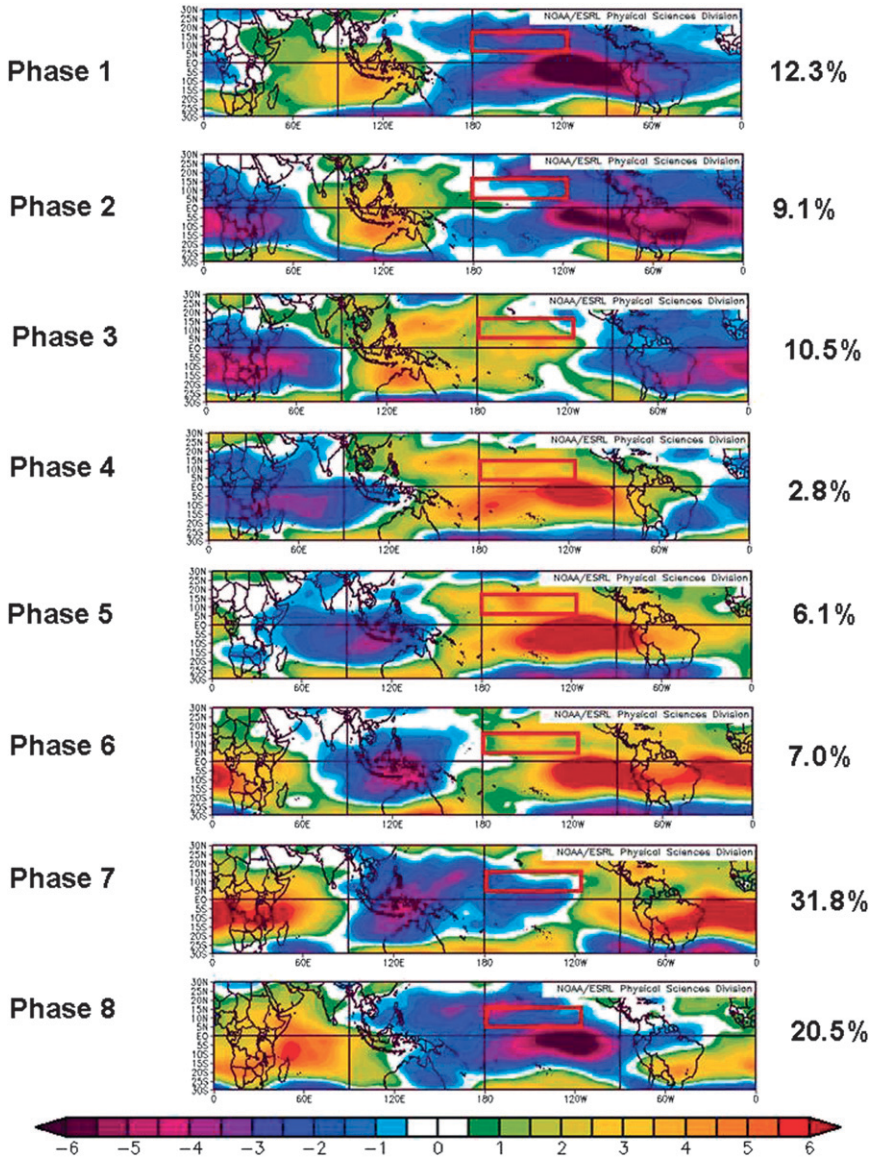

FIG. 4. As in Fig. 3, but for 200-mb U anomalies ($m\,s^{-1}$).

the Atlantic, where 54% of TCs that formed reach hurricane strength. A similar percentage of TCs (56%) reached hurricane strength in the eastern Pacific (east of 120°W). No significant trend is evident in north-central Pacific TC numbers.

Figure 2 displays the number of TCs forming by month during the north-central Pacific hurricane season from 15 May to 30 November. The most frequent month for TC formation in the north-central Pacific is August, when 40 out of 104 (38%) TCs developed. September is the second most active month of the season, followed by July. As can be seen from the figure, TC development is relatively unlikely in May and November. Only one TC has formed during each of these months.

The RI events in the north-central Pacific occur approximately at the same frequency for individual TCs as in the eastern Pacific and North Atlantic basins. For example, 34 out of 104 (33%) TCs that formed in the north-central Pacific had at least one RI event of 30 kt or greater. In comparison 36% of TCs forming in the eastern Pacific and Atlantic both had at least one RI event of 30 kt or greater, as calculated from the HURDAT database for the eastern Pacific (Davis et al. 1984) and the HURDAT database for the North Atlantic (Jarvinen et al. 1984).

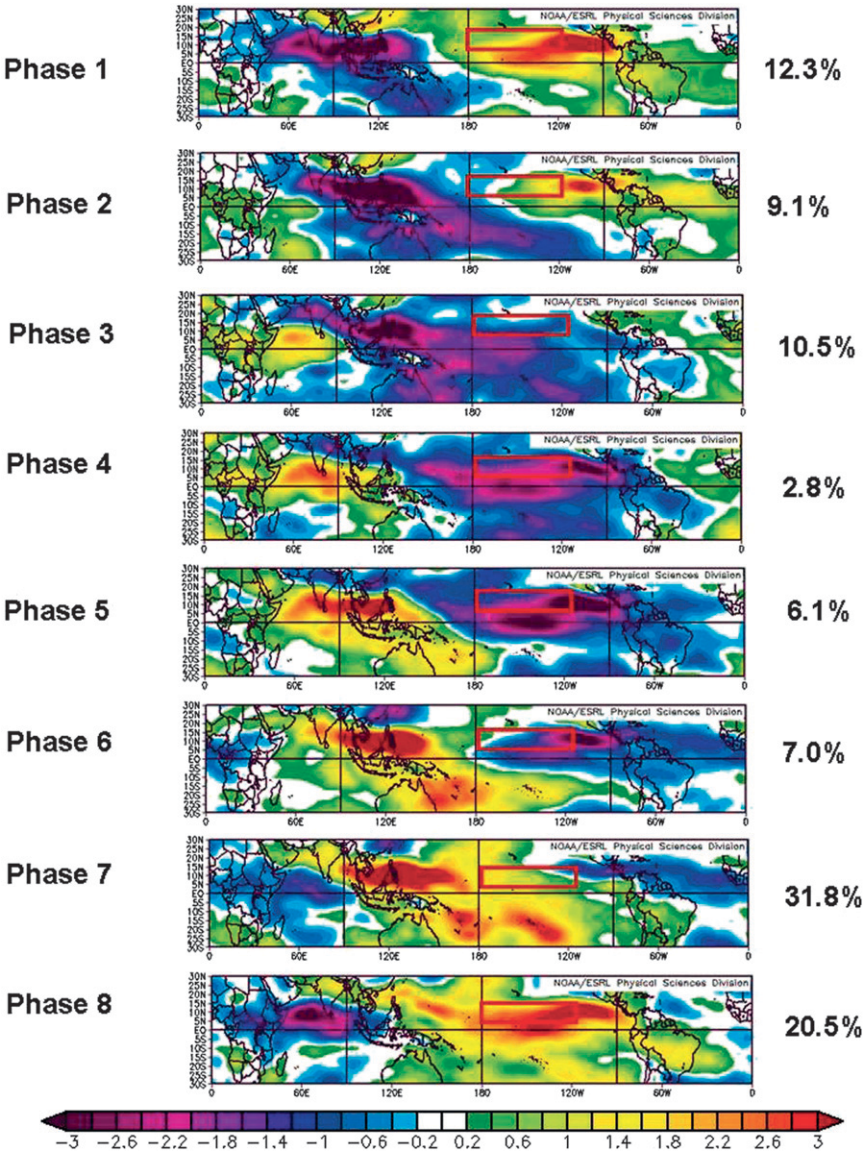

FIG. 5. As in Fig. 3, but for 850-mb U anomalies ($m\,s^{-1}$).

4. ENSO's modulation of TC activity in the north-central Pacific

From 1974 to 2010, the top 10 highest June–October-averaged MEI values were classified as El Niño events, the bottom 10 lowest June–October-averaged MEI values were classified as La Niña events, and all remaining years were classified as neutral. Results did not change significantly if slightly different ENSO thresholds were used. Table 1 displays the years classified as El Niño, neutral, and La Niña, respectively. The year 1978 was left out of this analysis, since OLR data are not available for calculating the MJO index that year. One of the goals of this research was to have a uniform dataset for comparing the MJO and ENSO's impacts on north-central Pacific TC activity.

Table 2 displays basinwide averages for the north-central Pacific MDR, defined as 8°–18°N, 180°–120°W, for various large-scale parameters in each ENSO phase as calculated by the NCEP–NCAR reanalysis from June to October. Averages are computed over these months (instead of 15 May–30 November 30), since only one TC formed between 15 and 30 May and one additional TC formed during November. Differences that are statistically significant at the 5% level using a two-tailed Student's t test are highlighted in boldface. Statistically significant differences are observed for SST, SLP, 700-mb relative humidity (RH), 300-mb omega, and

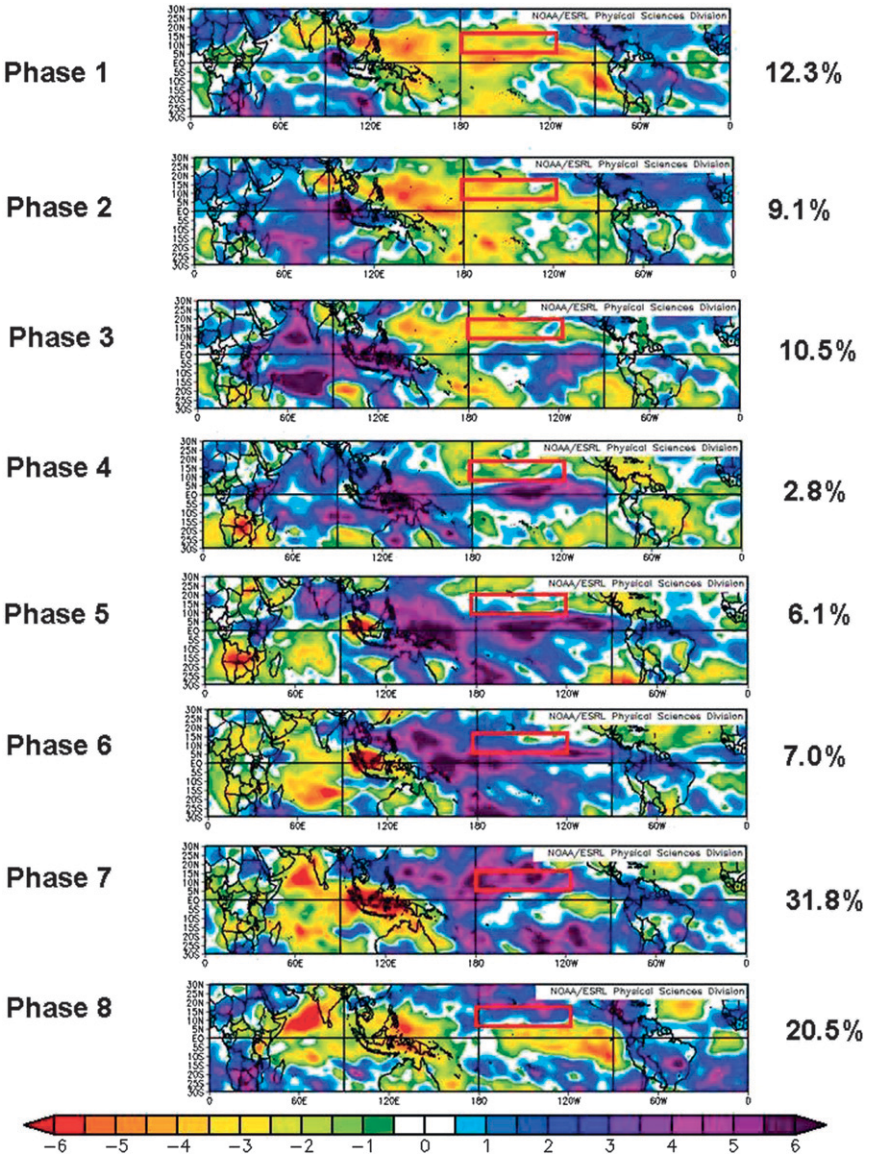

FIG. 6. As in Fig. 3, but for 700-mb RH anomalies (%).

OLR, indicating that a more favorable dynamic and thermodynamic environment generally exists in El Niño years in the north-central Pacific. The same fields are statistically significant at the 5% level using the WMW test.

Table 3 lists the average amount of activity occurring from TCs developing in the north-central Pacific in El Niño, neutral, and La Niña years, respectively. In general, TC activity in the north-central Pacific occurs more frequently in El Niño years, in keeping with the results of Clark and Chu (2002), Chu (2004), and Collins (2010). There appears to be very little difference in TC activity in the north-central Pacific between neutral and La Niña years, even though conditions appear to be somewhat more favorable for TC formation in neutral years (but not statistically significantly so). Statistically significant differences at the 10% level using the Student's *t* test are observed for all TC parameters between El Niño and La Niña years, except for major hurricanes and major hurricane days. These results are also significant at the 10% level for the same TC parameters when the WMW test is utilized.

While many more RI episodes are noted for El Niño years than for all other years (not shown), these differences are primarily related to more named storms in El Niño years. The chance of a TC forming in El Niño years versus all other years undergoing RI episodes of various magnitudes does not change significantly (Table 4).

TABLE 7. The average number of 24-h RI episodes of 25+, 30+, 35+, and 40+ kt experienced in phases 7 and 8 and phases 4 and 5, respectively. The percentage chance of a TC forming in either of these phase combinations undergoing at least one RI of these magnitudes is also displayed.

	RI (25+ kt)	RI (30+ kt)	RI (35+ kt)	RI (40+ kt)
Phases 7 and 8	7.2	5.0	3.8	1.9
Phases 4 and 5	0.3	0.0	0.0	0.0
Phases 7 and 8 (RI chance)	59%	41%	35%	18%
Phases 4 and 5 (RI chance)	8%	0%	0%	0%

5. MJO's modulation of TC activity in the north-central Pacific

Camargo et al. (2009) has documented the impacts of the MJO on various TC basins around the globe; however, to the authors' knowledge, no study has specifically focused on the MJO's impacts on north-central Pacific TCs. Table 5 displays TC activity generated by storms forming in each phase of the MJO. TC statistics are normalized by the number of days that the MJO spent in each phase from June to October, as the MJO preferentially spends more time in certain phases of the WH MJO index than others (e.g., Ventrice et al. 2011; Klotzbach 2012). Normalized values are multiplied by 100, so one can interpret the table as how much TC activity is typically generated per 100 days of each MJO phase. Phases 7 and 8 have the largest levels of TC activity, while phases 4 and 5 tend to have the lowest levels of TC activity. Differences are significant at the 10% level for all TC statistics except for MHD. When the WMW test is utilized, differences are significant at the 5% level for hurricanes and hurricane days, while all other fields except for named storm days are significant at between the 10% and 20% levels. The most TC-favored phases for the north-central Pacific are shifted slightly from the northeast Pacific (8°–18°N, 120°–90°W), where phases 8–1 tend to be the most conducive (not shown). For example, TCs forming in phase 7 in the north-central Pacific are responsible for 32% of all ACE generated in the basin, while TCs forming in phase 7 in the northeast Pacific are only responsible for 13% of all ACE generated in the basin.

Table 6 displays June–October-averaged conditions over the north-central Pacific MDR for each phase of the MJO as a difference from the average of all days during the June–October period. Statistically significant differences between phases 7 and 8 and phases 4 and 5 at the 5% level are highlighted in boldface type. Phases 7 and 8 have a statistically significant reduction in 200–850-mb zonal wind shear as well as an increase in 700-mb relative humidity when compared with phases 4 and 5, implying a more favorable thermodynamic and dynamic environment for TC formation in phases 7 and 8. Results remain significant at the same level when the WMW test is utilized.

Figure 3 displays upper-level velocity potential anomalies for the eight phases of the WH-MJO index. Also displayed on the right-hand side of the figure is the normalized percentage of basinwide ACE generated by TCs forming in each phase of the MJO. In general, TC activity is enhanced in phases slightly lagging the peak in velocity potential anomalies, which is similar to results found for the Atlantic basin (Klotzbach 2012). Typically, anomalies in the lower- and upper-level wind fields slightly lag those found in the velocity potential field (Figs. 4 and 5). Anomalous westerlies at low levels and anomalous easterlies at upper levels (counteracting the prevailing climatological westerly winds at upper level and easterly winds at lower levels) reduce westerly vertical wind shear in

TABLE 8. The TC activity generated by storms forming in each phase of the WH-Combined index. All values are normalized by the number of days that the MJO spends in a particular phase for June–October 1974–2010 and are multiplied by 100. All differences between phase 7 and the remaining phases of the WH-Combined index are statistically significant different at the 5% level.

Phase	NS	NSD	H	HD	MH	MHD	ACE
1	1.6	6.4	0.9	2.8	0.5	0.7	12.3
2	0.3	2.1	0.2	1.4	0.2	0.5	4.5
3	1.1	4.7	0.9	2.0	0.2	0.3	7.2
4	1.0	1.4	0.0	0.0	0.0	0.0	0.8
5	1.5	6.9	0.6	2.0	0.4	0.5	10.1
6	1.8	3.4	0.0	0.0	0.0	0.0	2.6
7	4.6	18.4	2.7	8.1	1.6	2.8	35.3
8	2.6	11.4	1.0	4.1	0.0	0.0	14.6
Average	1.8	6.8	0.8	2.5	0.4	0.6	10.9
Phase 7	4.6	18.4	2.7	8.1	1.6	2.8	35.3
All other phases	1.4	5.2	0.5	1.8	0.2	0.3	7.4
Phase 7/all other phases ratio	3.2	3.6	5.3	4.6	9.3	9.8	4.7

TABLE 9. As in Table 6, but for each phase of the WH-Combined index. Differences between phase 7 and the other phases that are statistically significant at the 5% level are highlighted in boldface type in the difference row.

MJO phase	SST	SLP	200-mb *U*	850-mb *U*	200–850-mb *U*	700-mb RH	500-mb omega	OLR
1	0.02	0.18	−2.71	1.35	−4.06	−0.99	5.46	7.06
2	−0.18	0.53	−2.60	0.75	−3.34	−2.79	4.29	7.65
3	−0.26	0.44	0.46	−0.45	0.91	−3.32	2.41	5.54
4	−0.19	0.09	2.62	−1.51	4.13	−1.61	−2.97	−1.44
5	0.04	−0.37	2.82	−1.57	4.39	1.13	−7.27	−7.69
6	0.14	−0.36	1.98	−0.67	2.65	2.93	−5.49	−8.39
7	0.31	−0.41	−1.87	0.87	−2.74	5.47	−0.83	−4.99
8	0.28	−0.31	−1.05	1.79	−2.84	0.94	4.41	0.83
Phase 7	0.31	−0.41	−1.87	0.87	−2.74	5.47	−0.83	−4.99
All other phases	−0.02	0.03	0.22	−0.04	0.26	−0.53	0.12	0.51
Phase 7 − all other phases	**0.34**	**−0.43**	−2.08	**0.92**	**−3.00**	**6.00**	−0.95	**−5.50**

phases 7 and 8 across the north-central Pacific MDR. This difference in vertical wind shear is likely one of the primary reasons why TC activity is enhanced in phases 7 and 8. Figure 6 displays 700-mb RH anomalies across the tropics, with enhanced RH observed across the north-central Pacific MDR in phases 7 and 8.

Table 7 displays how the MJO impacts the number of 24-h episodes of RI in the north-central Pacific basin. The table focuses on differences between phases 7 and 8 and phases 4 and 5, with activity in the intervening phases being between the levels shown between phases 7 and 8 and phases 4 and 5. Very large ratios are demonstrated between phases 7 and 8 and phases 4 and 5, with no RI episode of 30+ knots taking place since 1974 when a TC forms in the north-central Pacific and the MJO is in phases 4 and 5 (with an amplitude > 1). In addition, the chances of a TC undergoing RI are much greater for TCs forming in phases 7 and 8 than in phases 4 and 5.

6. Impacts of a combined MJO–ENSO index on TC activity in the north-central Pacific

The last two sections have documented that both ENSO and the MJO impact TC activity in the north-central Pacific. This section investigates the WH-Combined index to see if additional skill can be gathered by using this index, in a similar manner to what was done in Klotzbach (2012). Table 8 presents the normalized activity generated by TCs forming in each phase of the WH-Combined index. Phase 7 clearly stands out as the most active phase for north-central Pacific TC activity, with over 2.5 times more ACE generated in phase 7 than in the second most active phase (phase 8). Phase 7 has significantly more TC activity at the 5% level for all indices examined here when compared with the average of all other WH-Combined phases. To accurately run a WMW test, approximately even sample sizes of days must be compared, and consequently the differences between phases 4 and 5 and phases 7 and 8 are examined. Differences are significant at the 5% level for all TC statistics, except for MH and MHD, which are significant at the 10% level.

Table 9 displays June–October-averaged anomalous conditions over the north-central Pacific MDR for each phase of the WH-Combined index. Statistically significant differences at the 5% level are observed for 850-mb zonal wind, 200–850-mb zonal wind shear, SST, SLP, 700-mb RH, and OLR between phase 7 and the remaining MJO-Combined phases. All deviations are favorable for TC development. All deviations remain statistically significant at the 10% level when the WMW test is utilized. It appears that phase 7 has the best optimized combination of favorable thermodynamic and dynamic conditions in the north-central Pacific MDR.

TABLE 10. The average number of 24-h RI episodes of 25+, 30+, 35+, and 40+ kt experienced in phase 7 compared with the remaining phases (1–6, 8) of the WH-Combined index. All values are normalized by the number of days that the WH-Combined index spends in a particular phase for June–October 1974–2010 and are multiplied by 100. The ratio between phase 7 and the other seven phases is also provided. All differences are statistically significant at the 5% level except for an RI of 40+ kt, which is significant at the 10% level. The percentage chance of TCs forming in phase 7 of the WH-Combined index vs the other seven phases is included.

	RI (25+ kt)	RI (30+ kt)	RI (35+ kt)	RI (40+ kt)
Phase 7	13.5	8.6	6.5	3.0
Phases 1–6, 8	1.4	0.6	0.3	0.2
Ratio	9.8	13.8	19.8	14.2
Phase 7 (RI chance) (%)	65	59	47	18
Phases 1–6, 8 (RI chance) (%)	27	16	9	7

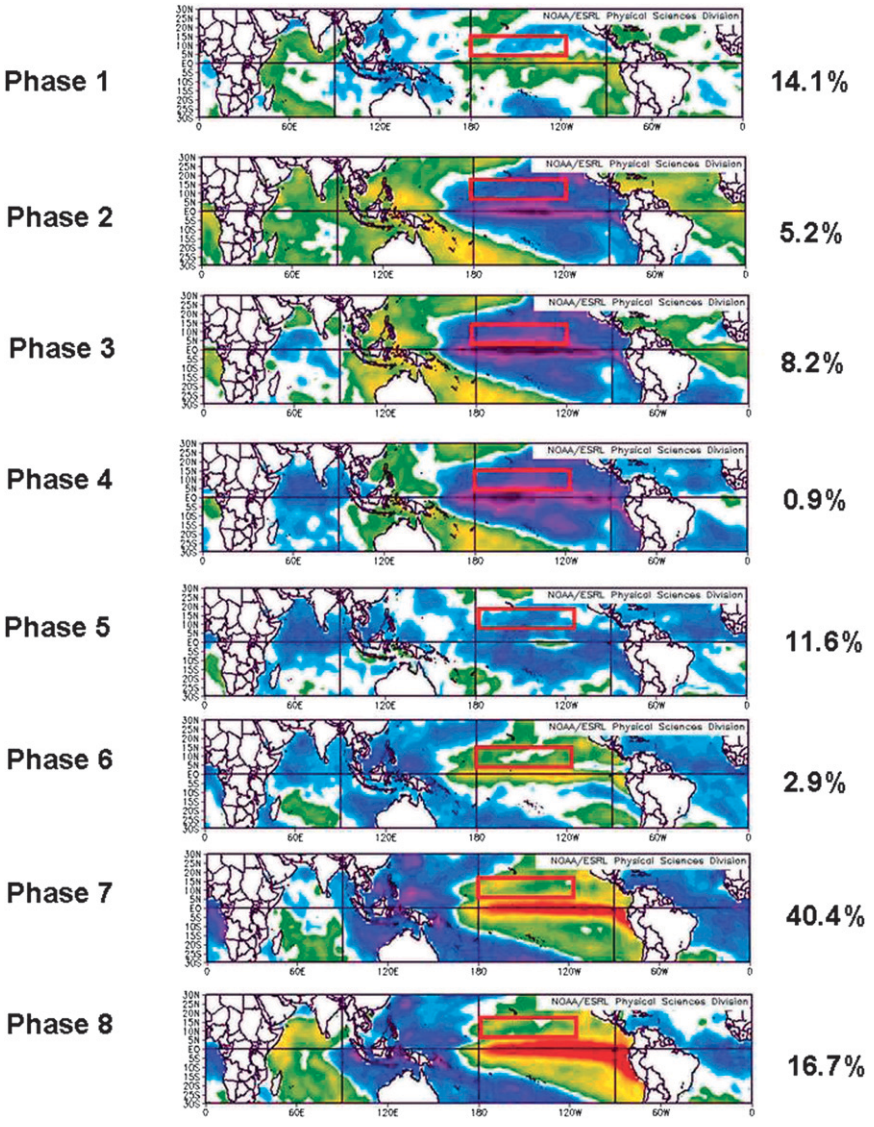

FIG. 7. Sea surface temperature anomalies (°C) for all days for June–October when the WH-Combined index was greater than one for (from top to bottom) each phase of the index. Numbers on the rhs represent the percentage of normalized ACE generated by TCs forming in each phase of the WH-Combined index. The red box represents the north-central Pacific MDR (8°–18°N, 180°–120°W).

Very strong differences are also observed for RI episodes. Table 10 displays the number of normalized 24-h periods for RI thresholds of 25 to 40 kt experienced in phase 7, compared with the remaining phases (phases 1–6 and 8) of the WH-Combined index. Phase 7 dominates RI episodes, with a statistically significant increase (at the 5% level) in the number of RI episodes for phase 7 compared with all other phases observed for all RI thresholds, except for 40+ knots. Similarly to what was done for overall TC activity, phases 4 and 5 and phases 7 and 8 are compared for the WMW test. Phases 7 and 8 have significantly more RI episodes at the 5% level for all RI thresholds. In addition, the likelihood of TCs undergoing an RI episode at some point during their lifetime is greater in phase 7 than in the average of all other phases.

The upper-level velocity potential anomalies for the WH-Combined index look very similar to those for the WH-MJO index (not shown). The most significant difference between the two indices seems to be in the SST field. Since the WH-Combined index includes ENSO, SSTs tend to be the warmest in the north-central Pacific

TABLE 11. Percentage of days that the WH-Combined index had an amplitude greater than one std dev for El Niño, neutral, and La Niña years, respectively.

	El Niño	Neutral	La Niña
1	11	14	9
2	3	15	30
3	3	9	24
4	3	13	22
5	12	18	10
6	20	15	2
7	25	7	1
8	24	9	1

in phase 7 as well (Fig. 7). This provides a more favorable thermodynamic environment for disturbances attempting to form in the north-central Pacific, which is the likely reason for the stronger signal evident in the WH-Combined index compared with the MJO index in isolation.

While the use of the WH-Combined index does appear to provide a stronger signal, the combined index can lose a considerable amount of the MJO-related signal for El Niño or La Niña events. Table 11 displays the percentage of days during June–October that the WH-Combined index is greater than one standard deviation for each phase of ENSO. For example, in La Niña years, the WH-Combined index is 76% of the time in phases 2–4, while it is only 9% of the time in phases 2–4 in El Niño years. Consequently, examining both an MJO index as well as an MJO–ENSO index in combination is critical when assessing the likelihood of TC formation in the north-central Pacific.

7. Summary and future work

This paper investigates the relationship among the MJO, ENSO, and north-central Pacific TC activity. In keeping with previous research, El Niño events are documented to increase north-central Pacific TC activity levels. Both thermodynamic and dynamic variables are shown to be more conducive for north-central Pacific TC formation in El Niño years when compared with neutral and La Niña years. Neutral and La Niña TC activities are not significantly different from each other. When anomalous subsidence associated with the MJO is located over the Indian Ocean (MJO phases 7 and 8), TC activity increases significantly in the north-central Pacific when compared with when the anomalously enhanced vertical motion associated with the MJO is located over the western Pacific (MJO phases 4 and 5). These impacts appear to be primarily associated with a more favorable vertical shear environment, with MDR-averaged vertical shear over $5\,m\,s^{-1}$ weaker in MJO phases 7 and 8 when compared with MJO phases 4 and 5. RI episodes are also shown to occur more frequently, and the chances of RI for a particular system increase, when the MJO is in phases 7 and 8. When an index combining the MJO and ENSO is utilized, even larger differences are seen for both TC activity in general and for RI.

The WH-Combined index has now been shown to be a powerful tool for both determining TC activity levels in the north-central Pacific as well as the Atlantic (Klotzbach 2012). This knowledge has the potential to be used in subseasonal forecasts for both basins. In the future, the authors plan to investigate the impact of the WH-Combined index on other TC basins, as well as investigating other causes of subseasonal TC variability in the north-central Pacific. In addition, changes in MJO-related impacts on north-central Pacific TCs on decadal time scales will be investigated, given the findings of Chu and Zhao (2004) that a significant change in TC activity on a decadal time scale occurred in the central Pacific during the early 1980s.

Acknowledgments. Valuable discussions on ENSO, the MJO, and its relationships with north-central Pacific TC were held with William Gray and Eric Maloney. Comments that significantly improved an earlier version of this manuscript were provided by Chris Landsea, Stacey Stewart, and four anonymous reviewers.

REFERENCES

Aiyyer, A., and J. Molinari, 2008: MJO and tropical cyclogenesis in the Gulf of Mexico and eastern Pacific: Case study and idealized numerical modeling. *J. Atmos. Sci.,* **65,** 2691–2704.

Barrett, B. S., and L. M. Leslie, 2009: Links between tropical cyclone activity and Madden–Julian oscillation phase in the North Atlantic and northeast Pacific basins. *Mon. Wea. Rev.,* **137,** 727–744.

Bell, G. D., and Coauthors, 2000: Climate assessment for 1999. *Bull. Amer. Meteor. Soc.,* **81,** S1–S50.

Camargo, S. J., K. A. Emanuel, and A. H. Sobel, 2007: Use of a genesis potential index to diagnose ENSO effects on tropical cyclone genesis. *J. Climate,* **20,** 4819–4834.

——, M. C. Wheeler, and A. H. Sobel, 2009: Diagnosis of the MJO modulation of tropical cyclogenesis using an empirical index. *J. Atmos. Sci.,* **66,** 3061–3074.

Chu, P.-S., 2004: ENSO and tropical cyclone activity. *Hurricanes and Typhoons: Past, Present, and Future,* R. J. Murnane and K.-B. Liu, Eds., Columbia University Press, 297–332.

——, and X. Zhao, 2004: Bayesian change-point analysis of tropical cyclone activity: The central North Pacific case. *J. Climate,* **17,** 4893–4901.

Clark, J. D., and P.-S. Chu, 2002: Interannual variation of tropical cyclone activity over the central North Pacific. *J. Meteor. Soc. Japan,* **80,** 403–418.

Collins, J. M., 2010: Contrasting high northeast Pacific tropical cyclone activity with low North Atlantic activity. *Southeast. Geogr.,* **50,** 83–98.

Davis, M. A. S., G. M. Brown, and P. Leftwich, 1984: A tropical cyclone data tape for the eastern and central North Pacific

basins, 1949–1983: Contents, limitations, and uses. NOAA Tech. Memo. NWS NHC 25, 17 pp.

Gray, W. M., 1979: Hurricanes: Their formation, structure and likely role in the tropical circulation. *Meteorology over Tropical Oceans,* D. B. Shaw, Ed., Royal Meteorological Society, 155–218.

——, and J. D. Sheaffer, 1991: El Niño and QBO influences on tropical cyclone activity. *Teleconnections Linking Worldwide Anomalies,* M. H. Glantz, R. W. Katz, and N. Nicholls, Eds., Cambridge University Press, 257–284.

Jarvinen, B. R., C. J. Neumann, and M. A. S. Davis, 1984: A tropical cyclone data tape for the North Atlantic basin, 1886–1983: Contents, limitations, and uses. NOAA Tech. Memo. NWS NHC 22, 21 pp.

Kistler, R., and Coauthors, 2001: The NCEP–NCAR 50-Year Reanalysis: Monthly means CD-ROM and documentation. *Bull. Amer. Meteor. Soc.,* **82,** 247–267.

Klotzbach, P. J., 2012: El Niño–Southern Oscillation, the Madden–Julian oscillation and Atlantic basin tropical cyclone rapid intensification. *J. Geophys. Res.,* **117,** D14104, doi:10.1029/2012JD017714.

——, and W. M. Gray, 2003: Forecasting September Atlantic basin tropical cyclone activity. *Wea. Forecasting,* **18,** 1109–1128.

Liebmann, B., and C. A. Smith, 1996: Description of a complete (interpolated) outgoing longwave radiation dataset. *Bull. Amer. Meteor. Soc.,* **77,** 1275–1277.

Madden, R. A., and P. R. Julian, 1972: Description of global-scale circulation cells in the tropics with a 40–50 day period. *J. Atmos. Sci.,* **29,** 1109–1123.

Maloney, E. D., and D. L. Hartmann, 2000: Modulation of eastern North Pacific hurricanes by the Madden–Julian oscillation. *J. Climate,* **13,** 1451–1460.

Rasmussen, E. M., and T. H. Carpenter, 1982: Variations in tropical sea surface temperature and surface wind fields associated with the Southern Oscillation/El Niño. *Mon. Wea. Rev.,* **110,** 354–384.

Ventrice, M. J., C. D. Thorncroft, and P. E. Roundy, 2011: The Madden–Julian oscillation's influence on African easterly waves and downstream tropical cyclogenesis. *Mon. Wea. Rev.,* **139,** 2704–2722.

Wang, C., 2005: ENSO, Atlantic climate variability, and the Walker and Hadley circulations. *The Hadley Circulation: Past, Present, and Future,* H. F. Diaz and R. S. Bradley, Eds., Kluwer Academic, 173–202.

Wheeler, M. C., and H. H. Hendon, 2004: An all-season real-time multivariate MJO index: Development of an index for monitoring and prediction. *Mon. Wea. Rev.,* **132,** 1917–1932.

Wolter, K., and M. S. Timlin, 1998: Measuring the strength of ENSO events—How does 1997/98 rank? *Weather,* **53,** 315–324.